

See discussions, stats, and author profiles for this publication at: <https://www.researchgate.net/publication/5396296>

Solventless Adhesive Bonding Using Reactive Polymer Coatings

ARTICLE *in* ANALYTICAL CHEMISTRY · JULY 2008

Impact Factor: 5.64 · DOI: 10.1021/ac800341m · Source: PubMed

CITATIONS

51

READS

81

4 AUTHORS, INCLUDING:



Arthur McClelland

Harvard University

15 PUBLICATIONS 147 CITATIONS

SEE PROFILE

Solventless Adhesive Bonding Using Reactive Polymer Coatings

Hsien-Yeh Chen,[†] Arthur A. McClelland,^{||} Zhan Chen,^{§,⊥} and Joerg Lahann^{*,†,‡,§}

Departments of Chemical Engineering, Materials Science and Engineering, Macromolecular Science and Engineering, Applied Physics, and Chemistry, University of Michigan, Ann Arbor, Michigan 48109

A novel solventless adhesive bonding (SAB) process is reported, which is applicable to a wide range of materials including, but not limited to, poly(dimethylsiloxane) (PDMS). The bonding is achieved through reactions between two complementary polymer coatings, poly(4-aminomethyl-*p*-xylylene-*co-p*-xylylene) and poly(4-formyl-*p*-xylylene-*co-p*-xylylene), which are prepared by chemical vapor deposition (CVD) polymerization of the corresponding [2.2]paracyclophanes and can be deposited on complementary microfluidic units to be bonded. These CVD-based polymer films form well-adherent coatings on a range of different substrate materials including polymers, glass, silicon, metals, or paper and can be stored for extended periods prior to bonding without losing their bonding capability. Tensile stress data are measured on PDMS with various substrates and compared favorably to current methods such as oxygen plasma and UV/ozone. Sum frequency generation (SFG) has been used to probe the presence of amine and aldehyde groups on the surface after CVD polymerization and their conversion during bonding. In addition to bonding, unreacted functional groups present on the luminal surface of microfluidic channels provide free chemical groups for further surface modification. Fluorescently labeled molecules including rhodamine-conjugated streptavidin and atto-655 NHS ester were used to verify the presence of active functional groups on the luminal surfaces after bonding.

Rapid progress in biotechnology and related fields has fueled the need for progressively miniaturized devices with increasing biological complexity.^{1–6} This trend has led to a cross-fertilization

between biology, materials science, and chemistry that has provided novel materials and advanced microfluidic device fabrication processes, which can be precisely tailored toward specific biotechnological requirements. Along with the introduction of novel materials and device architectures came a series of challenges, many of which are related to device integration. For the fabrication of miniaturized devices with use in biotechnology, effective bonding of independently designed substructures has emerged as a major challenge. Current bonding methodologies include direct bonding, adhesive bonding, anodic bonding, solder or eutectic bonding, as well as thermo-compression bonding, but these methods are often limited to a specific substrates or involve the application of additional bonding chemicals or require harsh process conditions.^{7,8} For instance, bonding of poly(dimethylsiloxane) (PDMS) is widely used for low-cost biotechnological applications but requires oxidative pretreatment, such as oxygen plasma^{9–12} or UV/ozone¹³ activation. Upon exposure to highly oxidative environments, silanol groups are created, which can result in strong intermolecular bonding.¹² In most of the cases, the oxidative activation effects are temporary due to hydrophobic recovery,¹⁵ and the oxidation reaction must be conducted immediately prior to bonding. Hydrophobic recovery may be slowed down by storage in water or extraction of low molecular weight components.^{7,13,14} In addition, these approaches are limited to a small group of substrates, such as PDMS, silicon, or glass, impeding the use for more complex devices that may be constructed of a number different materials. To date, further progress has been limited by the lack of precision in the chemical reactions used for bonding, which often require empirical process optimization. These challenges have not only been witnessed in biotechnological applications but also in many chemical and electronic device applications.

* To whom correspondence should be addressed. E-mail: lahann@umich.edu.

[†] Chemical Engineering.

[‡] Materials Science and Engineering.

[§] Macromolecular Science and Engineering.

^{||} Applied Physics.

[⊥] Chemistry.

- (1) Tian, J. D.; Gong, H.; Sheng, N. J.; Zhou, X. C.; Gulari, E.; Gao, X. L.; Church, G. *Nature* **2004**, *432*, 1050–1054.
- (2) Pellois, J. P.; Zhou, X. C.; Srivannavit, O.; Zhou, T. C.; Gulari, E.; Gao, X. L. *Nat. Biotechnol.* **2002**, *20*, 922–926.
- (3) Lucchetta, E. M.; Lee, J. H.; Fu, L. A.; Patel, N. H.; Ismagilov, R. F. *Nature* **2005**, *434*, 1134–1138.
- (4) Petty, R. T.; Li, H. W.; Maduram, J. H.; Ismagilov, R.; Mrksich, M. J. *Am. Chem. Soc.* **2007**, *129*, 8966–8967.
- (5) Berg, A.; Olthius, W.; Bergveld, P. *Micro Total Analysis Systems 2000*, 1st ed.; Springer, 2000.
- (6) Fu, A. Y.; Spence, C.; Scherer, A.; Arnold, F. H.; Quake, S. R. *Nat. Biotechnol.* **1999**, *17*, 1109–1111.

- (7) Chen, C. S.; Mrksich, M.; Huang, S.; Whitesides, G. M.; Ingber, D. E. *Science* **1997**, *276*, 1425–1428.
- (8) Harrison, C.; Cabral, J.; Stafford, C. M.; Karim, A.; Amis, E. J. *J. Microelectromech. Syst.* **2004**, *14*, 153–158.
- (9) Niklaus, F.; Stemme, G.; Lu, J. Q.; Gutmann, R. J. *J. Appl. Phys.* **2006**, *99*, 031101–031128.
- (10) McDonald, J. C.; Duffy, D. C.; Anderson, J. R.; Chiu, D. T.; Wu, H. K.; Schueller, O. J. A.; Whitesides, G. M. *Electrophoresis* **2000**, *21*, 27–40.
- (11) Duffy, D. C.; McDonald, J. C.; Schueller, O. J. A.; Whitesides, G. M. *Anal. Chem.* **1998**, *70*, 4974–4984.
- (12) Bhattacharya, S.; Datta, A.; Berg, J. M.; Gangopadhyay, S. *J. Microelectromech. Syst.* **2005**, *14*, 590–597.
- (13) McDonald, J. C.; Whitesides, G. M. *Acc. Chem. Res.* **2002**, *35*, 491–499.
- (14) Cygan, Z. T.; Cabral, J. T.; Beers, K. L.; Amis, E. J. *Langmuir* **2005**, *21*, 3629–3634.
- (15) Makamba, H.; Kim, J. H.; Lim, K.; Park, N.; Hahn, J. H. *Electrophoresis* **2003**, *24*, 3607–3619.

As a consequence, tailored surface reactions have recently generated intense attention in modifying the surfaces of microfluidic devices and for protein immobilization.^{16–18} Among the most promising candidates are chemical processes that ensure selective conversions and high thermodynamic driving forces, while minimizing the risk of undesired side reactions. A prime example of a highly efficient and orthogonal reaction is the so-called click chemistry^{19,20} that has been rapidly embraced by the materials community.^{19–22} We now propose an alternate strategy for chemical bonding, the solventless adhesive bonding (SAB) process, which relies on reactive polymer coatings with precisely engineered surface chemistries and is applicable to a wide range of materials including, but not limited to, PDMS. In addition, we elucidate the exact molecular mechanism of the SAB process using sum frequency generation (SFG) spectroscopy. Because of the high selectivity of the chemistry exploited for SAB, the process lends itself to simultaneous bonding and surface modification.

EXPERIMENTAL SECTION

Materials. PDMS samples were prepared by uniformly mixed PDMS prepolymer and curing agent (Sylgard 184, Dow Corning) at a ratio of 10:1 and were cured at 70 °C for 1 h.¹³ Glass slides (Fisher), poly(tetrafluoroethylene) (PTFE) films (0.01 mm, Goodfellow), and stainless steel foils (AISI 316L–Fe/Cr18/Ni10/Mo3, annealed, 0.1 mm, Goodfellow) were used as received. Gold samples were prepared on silicon wafers (Silicon Valley Microelectronics, Inc.) by e-beam deposition, with 3 nm of titanium followed by 80 nm of gold.

Chemical Vapor Deposition Polymerization of Poly(*p*-xylylenes). Poly(4-aminomethyl-*p*-xylylene)-*co*-(*p*-xylylene) (**1**) and poly(4-formyl-*p*-xylylene-*co*-*p*-xylylene) (**2**) were synthesized via chemical vapor deposition (CVD) polymerization in a custom-made CVD polymerization system.²³ The starting materials, 4-aminomethyl[2,2]paracyclophane or 4-formyl[2,2]paracyclophane, were sublimed under vacuum and converted by pyrolysis into the corresponding quinodimethanes, which spontaneously polymerized upon condensation to the cooled substrate surface, which was maintained at 15 °C. Throughout CVD polymerization, a constant argon flow of 20 sccm and a working pressure of 0.5 mbar were maintained. The pyrolysis temperature was set to be 700 °C, and sublimation temperatures were between 90 and 110 °C under these conditions. CVD polymerization spontaneously occurred on samples placed on a rotating, cooled sample holder.

Surface Characterization. Film thicknesses were measured using a multiwavelength rotating analyzer ellipsometer (M-44, J. A. Woollam) at an incident angle of 75°. The data were analyzed using WVASE32 software. Thickness measurements were recorded by fitting the ellipsometric ψ and δ data with $An = 1.65$,

$Bn = 0.01$ for polymer **1** and $An = 1.76$, $Bn = 0.01$ for polymer **2** using a Cauchy model and software module integrated with the system. SFG spectra were recorded by using a pulsed visible laser beam and a tunable pulsed infrared beam that are overlapped spatially and temporally on sample surfaces at incident angles of 60° and 45°, with pulse energies of ~ 200 and ~ 100 μ J, respectively. Unless otherwise specified, all SFG spectra were recorded by ssp (s-polarized sum frequency output, s-polarized visible input, and p-polarized IR input) polarization combination and were normalized by the intensities of input visible and IR beams. The details of the SFG setup and experimental geometry were detailed elsewhere.^{24–28}

Bonding Process and Tensile Stress Test. The SAB process was performed by first coating substrates with polymers **1** or **2**. After coating, samples were brought into contact and were then placed in an oven at 140 °C for 3 h. The resulting samples were tested and stored at room temperature (20 °C). UV/ozone bonding was performed by using a UVO cleaner (model 342, Jelight Co.) treating the substrates for 30 min. The resulting samples were then cured at 120 °C for 20 min. Oxygen plasma bonding was performed by using a plasma etcher (SPI Plasma-Prep II, SPI Supplies/Structure Probe, Inc.). Treatment was done by using 10 W of energetic oxygen plasma under 200–300 mTorr pressure for 30 s. The plasma-treated samples were then cured at 60 °C for 10 min or 120 °C for 10 min. For all samples, tensile stress was tested using a Bionix 100 mechanical tester (MTS, Co.) equipped with a 10 N load sensor. Samples were prepared in a cross-sectional area of 10 mm \times 10 mm, and the measurement was recorded at a displacement rate of 0.05 mm/min.

Surface Immobilization. PDMS microchannels were fabricated using standard photolithography procedures described elsewhere²⁹ and were coated with polymer **2**. Commercially available cover glasses (25 mm \times 25 mm, Fisher) were used as received and were coated with polymer **1**. The CVD coated PDMS and cover glass were bonded via the SAB process. After bonding, the devices were first incubated with atto-655 NHS ester (50 μ g/mL, Fluka) in phosphate-buffered saline (PBS, pH 7.4) for 120 min and subsequently rinsed several times with PBS containing 0.1% (w/v) bovine albumin and Tween 20 (0.02% (v/v)). The resulting devices were then incubated with 20 mM biotin–hydrazide solution (Pierce Biotechnology, Inc.) in acidic condition (pH 3) for 5 min. Deionized water and PBS solution was used to separate unreacted biotin–hydrazide. The rinsed devices were incubated with rhodamine (TRITC)-conjugated streptavidin (50 μ g/mL, Pierce) in PBS containing 0.1% (w/v) bovine albumin and Tween 20 (0.02% (v/v)) for 90 min. Finally, samples were thoroughly rinsed with PBS containing 0.1% (w/v) bovine albumin and Tween 20 (0.02% (v/v)).

Fluorescence and Confocal Microscopy. Fluorescence images were visualized using a Nikon TE 200 fluorescent micro-

- (16) Quake, S. R.; Scherer, A. *Science* **2000**, *290*, 1536–1540.
- (17) Janasek, D.; Franzke, J.; Manz, A. *Nature* **2006**, *442*, 374–380.
- (18) Yoshida, M.; Langer, R.; Lendlein, A.; Lahann, J. *Polym. Rev.* **2006**, *46*, 347–375.
- (19) Diaz, D. D.; Punna, S.; Holzer, P.; McPherson, A. K.; Sharpless, K. B.; Fokin, V. V.; Finn, M. G. *J. Polym. Sci., Part A: Polym. Chem.* **2004**, *42*, 4392–4403.
- (20) Kolb, H. C.; Finn, M. G.; Sharpless, K. B. *Angew. Chem., Int. Ed.* **2001**, *40*, 2004–2021.
- (21) Lutz, J. F. *Angew. Chem., Int. Ed.* **2007**, *46*, 1018–1025.
- (22) Nandivada, H.; Jiang, X. W.; Lahann, J. *Adv. Mater.* **2007**, *19*, 2197–2208.
- (23) Chen, H. Y.; Lahann, J. *Anal. Chem.* **2005**, *77*, 6909–6914.

- (24) Chen, C.-Y.; Even, M. A.; Wang, J.; Chen, Z. *Macromolecules* **2002**, *35*, 9130–9135.
- (25) Loch, C. L.; Ahn, D.; Chen, C. Y.; Wang, J.; Chen, Z. *Langmuir* **2004**, *20*, 5467–5473.
- (26) Loch, C. L.; Ahn, D.; Chen, Z. *J. Phys. Chem. B* **2006**, *110*, 914–918.
- (27) Chen, C. Y.; Loch, C. L.; Wang, J.; Chen, Z. *J. Phys. Chem. B* **2003**, *107*, 10440–10445.
- (28) Wang, J.; Chen, C.; Buck, S. M.; Chen, Z. *J. Phys. Chem. B* **2001**, *105*, 12118–12125.
- (29) Chen, H. Y.; Lahann, J. *Adv. Mater.* **2007**, *19*, 3801–3808.

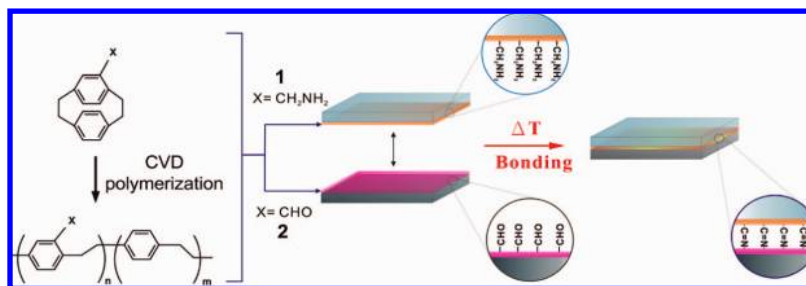


Figure 1. Schematic illustration of the solventless adhesive bonding (SAB) process. During SAB, formation of a strong adhesion layer is achieved by bonding of two complementary CVD reactive coatings **1** and **2**.

scope, 10× or 4× dry objectives were used, and a digital interline CCD camera (Cascade 512F, Roper Scientific) was controlled by the Metavue software (version 6.1r6). Three dimensional fluorescence images were captured by using a confocal laser scanning microscope (CLSM) (TCS SP2, Leica Microsystems, U.S.A.) on an inverted microscope (DMIRE2, Leica Microsystems, U.S.A.). A GreNe laser (wavelength 543 nm) and a HeNe laser (wavelength 633 nm) were used to excite tetramethylrhodamine isothiocyanate (TRITC)-labeled streptavidin and atto-655 NHS ester, respectively (www.atto-tec.de). The emission was confined to 560–595 nm for TRITC-labeled streptavidin and 650–700 nm for atto-655 NHS ester upon observation. Confocal *z*-stack imaging scanning was performed using a 2.5 μm pixel resolution in the *z*-direction.

RESULTS AND DISCUSSION

As shown in Figure 1, the SAB process uses two vapor-deposited reactive polymer coatings with complementary functional groups, which are amino and aldehyde groups in this example. The ultrathin adhesion layers are conformally applied to the substrates of choice using a coating technology recently developed in our group.^{30,31} Under the influence of moderately increased temperatures (about 140 °C), the polymer coatings react with each other with high affinity. In contrast, both coatings are relatively inert when stored at room temperature—allowing for bonding on demand. This feature is distinct from traditional PDMS bonding techniques, where the energy treatment has to be conducted immediately prior to bonding. In addition, CVD-based polymer films form well-adherent coatings on a range of different substrate materials including polymers, glass, silicon, metals, or paper and can be stored for extended periods prior to bonding without losing the bonding capability.^{32–36} In fact, reactive coatings used herein, poly(4-aminomethyl-*p*-xylylene-*co-p*-xylylene)^{37,38} (**1**) and poly(4-formyl-*p*-xylylene-*co-p*-xylylene)³³ (**2**), are stable under dry conditions until brought in contact with each other at elevated temperatures. Prior to mechanical testing, the chemical structures

Table 1. Experimental Tensile Stress Data

method	material	bonding strength (MPa)
SAB ^a	PDMS–PDMS	$>2.44 \pm 0.15^b$
SAB	PDMS–PTFE	1.21 ± 0.35
SAB ^a	PDMS–stainless steel	$>2.44 \pm 0.15$
SAB ^a	PDMS–silicon wafer	$>2.44 \pm 0.15$
SAB ^a	PDMS–glass	$>2.44 \pm 0.15$
SAB ^a	PDMS–gold	$>2.44 \pm 0.15$
physical contact	PDMS–PDMS	0.02 ± 0.11
heat (140 °C)	PDMS–PDMS	0.19 ± 0.09
UV/ozone	PDMS–PDMS	0.78 ± 0.08
oxygen plasma	PDMS–PDMS	2.34 ± 0.27
oxygen plasma (cured at 120 °C)		
oxygen plasma (cured at 60 °C)	PDMS–PDMS	1.15 ± 0.18

^a CVD coatings of **1** and **2** were used as examples. ^b Fracture strength of PDMS was 2.44 ± 0.15 MPa compared to 2.24 MPa reported in the Polymer Data Handbook (Mark, J. E. *Polymer Data Handbook*; Oxford University Press: New York, 1999).

of all polymer films were confirmed by X-ray photoelectron spectroscopy (XPS). Film thicknesses were in the range of 40–80 nm as measured by ellipsometry. Because this novel approach uses solventless polymer coatings, it eliminates the need for solvent-based adhesives as well as pretreatment steps that need to be applied immediately prior to bonding.

In a typical bonding experiment, a substrate coated with polymer **1** and a second substrate coated with polymer **2** were brought into conformal contact without applying additional pressure. The contacting samples were then placed in a 140 °C oven for at least 3 h. Adhesion was measured using a standard tensile stress experiment (Table 1),³⁹ using a Bionix 100 mechanical tester (MTS, Co.) equipped with a 10 N load sensor. For many of the tested substrate combinations described in Table 1, high bonding strengths were measured. When bonding two PDMS substrates coated with either polymer **1** or **2**, tensile stresses as high as 2.44 MPa were measured, which is identical to the fracture strengths of PDMS. Accordingly, rupture consistently occurred within one of the PDMS substrates and not at the bonding interface. Similar results were obtained when PDMS was bonded to stainless steel, silicon, or glass. When using the dry bonding approach to bond PDMS to PTFE (Teflon), bonding strengths averaged 1.21 MPa. These bonding strengths are comparable to those of samples bonded by plasma plus heat treatment, which was included in the study as reference, but higher than bonding data obtained without reactive coatings or simple plasma or UV/

- (30) Lahann, J. *Chem. Eng. Commun.* **2006**, *193*, 1457–1468.
- (31) Lahann, J.; Langer, R. *Macromolecules* **2002**, *35*, 4380–4386.
- (32) Nandivada, H.; Chen, H. Y.; Bondarenko, L.; Lahann, J. *Angew. Chem., Int. Ed.* **2006**, *45*, 3360–3363.
- (33) Nandivada, H.; Chen, H. Y.; Lahann, J. *Macromol. Rapid Commun.* **2005**, *26*, 1794–1799.
- (34) Suh, K. Y.; Langer, R.; Lahann, J. *Adv. Mater.* **2004**, *16*, 1401–1405.
- (35) Lahann, J.; Balcells, M.; Lu, H.; Rodon, T.; Jensen, K. F.; Langer, R. *Anal. Chem.* **2003**, *75*, 2117–2122.
- (36) Lahann, J.; Balcells, M.; Rodon, T.; Lee, J.; Choi, I. S.; Jensen, K. F.; Langer, R. *Langmuir* **2002**, *18*, 3632–3638.
- (37) Chow, W. W. Y.; Lei, K. F.; Shi, G. Y.; Li, W. J.; Huang, Q. *Smart Mater. Struct.* **2006**, *15*, S112–S116.
- (38) Elkasabi, Y.; Chen, H. Y.; Lahann, J. *Adv. Mater.* **2006**, *18*, 1521–1526.

- (39) Rozenberg, V. I.; Danilova, T. I.; Sergeeva, E. V.; Shouklov, I. A.; Starikova, Z. A.; Hopf, H.; Kuhllein, K. *Eur. J. Org. Chem.* **2003**, 432–440.

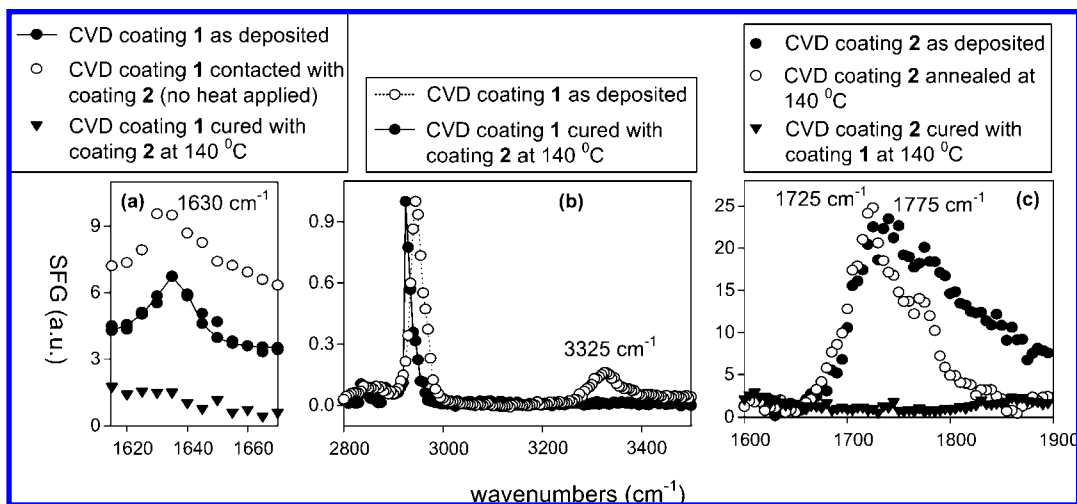


Figure 2. SFG spectra of polymers **1** and **2** before and after bonding. (a) SFG spectra of polymer **1** showing the presence of the characteristic NH_2 bending (coupled with the aromatic ring stretching) peak at 1630 cm^{-1} before bonding, which disappears after bonding. (b) SFG spectra of polymer **1** showing the presence of the characteristic N-H stretching peak at 3325 cm^{-1} before bonding. The signal disappears after bonding. (c) SFG spectra of polymer **2** showing the presence of characteristic C=O stretching peak before bonding.

ozone activated bonding. Although the group of reference materials included in this study is not exhaustive, it becomes evident that adhesion obtained with the SAB process clearly falls within a range required for many microfluidic applications. The use of CVD-based polymer coatings also effectively suppresses restructuring of otherwise quite dynamic PDMS surfaces. For example, a PDMS-based microchannel bound to a silicon substrate using the SAB methodology showed excellent adhesion after storage for more than 1 year under ambient conditions (air, medium humidity, varying temperatures between 20 and 25 °C).

To further elucidate the underlying mechanism of the bonding process at the molecular level, we used SFG spectroscopy. SFG provides details about the buried interface involving polymers^{24–28} and is well suited for investigating the adhesion layer formed between the two substrates. On the basis of a series of control experiments with CVD coatings that had different side groups, we hypothesized that covalent binding via imine bonds formed between CHO and CH_2NH_2 groups of the two polymer coatings. When a PDMS substrate coated with polymer **1** is initially brought in contact with a quartz substrate coated with polymer **2**, characteristic signals related to the primary amino groups of polymer **1** were detected at 1630 cm^{-1} (NH_2 bending coupled with aromatic ring stretching, Figure 2a) and 3325 cm^{-1} (N-H stretch, Figure 2b). Moreover, the characteristic C=O stretches (Figure 2c) of the aldehyde groups stemming from polymer **2** were detected at 1725 cm^{-1} . Prior to exposure to sufficiently high temperatures, the complementary chemical groups continue to coexist without detectable chemical conversion. After the substrate temperature was raised to 140 °C, however, both amines and aldehyde groups were simultaneously consumed as indicated by the disappearance of the characteristic signals at 1630 and 3325 cm^{-1} , on the one hand, and 1725 cm^{-1} on the other. Interestingly, these effects were not observed when the substrates were brought in contact without heating (Figure 2a) or when one coating alone was heated (Figure 2c), suggesting that the observed changes in the SFG spectra indeed correlate with the bonding event. On the

basis of these experiments, we concluded that the strong bonding is due to the chemical reaction between amino and aldehyde groups.

In addition to bonding, an important aspect of biological devices is the need for precise modification of the luminal surfaces of microchannels. CVD polymerization results in homogeneous coating of the entire surface of a device substructure. During thermal bonding, however, only functional groups that come in direct contact with the complementary surface chemistry will be consumed. Functional groups that are located within the microchannels and therefore are not exposed to complimentary functional groups remain—at least in principle—available for surface modification.

To address the question of whether polymer films deposited within microchannels still maintain their typical reactivity after the curing process, we conducted a series of immobilization studies in previously bonded devices. For this purpose, PDMS-based microchannels were fabricated using a standard procedure described previously.²⁹ Poly(4-formyl-*p*-xylylene-*co-p*-xylylene) (**2**) was deposited onto the resulting PDMS microchannels via CVD polymerization. Commercially available glass slides were coated with poly(4-aminomethyl-*p*-xylylene-*co-p*-xylylene) (**1**) via CVD polymerization. In this setting, the reactive coatings provide dual function: (i) they chemically bound the microchannels, where glass and PDMS are brought in direct contact to each other, and (ii) they provide free chemical groups for further surface modification on the luminal surfaces of the microchannels, which are conserved under the conditions of thermal bonding (Figure 3). Whereas polymer **1** provides primary amino groups for coupling with activated carboxyl groups (amide formation), polymer **2** has aldehyde groups that can react with hydrazines or hydrazides. After CVD modification, the PDMS microchannels and glass coverslips were brought in contact and bonded following the SAB process, as described before. To assess the chemical activity of the coating after exposure to the SAB process, hydrazide-derived biotin ligands were allowed to react with the functional groups present within the microchannels. The biotin ligand was chosen

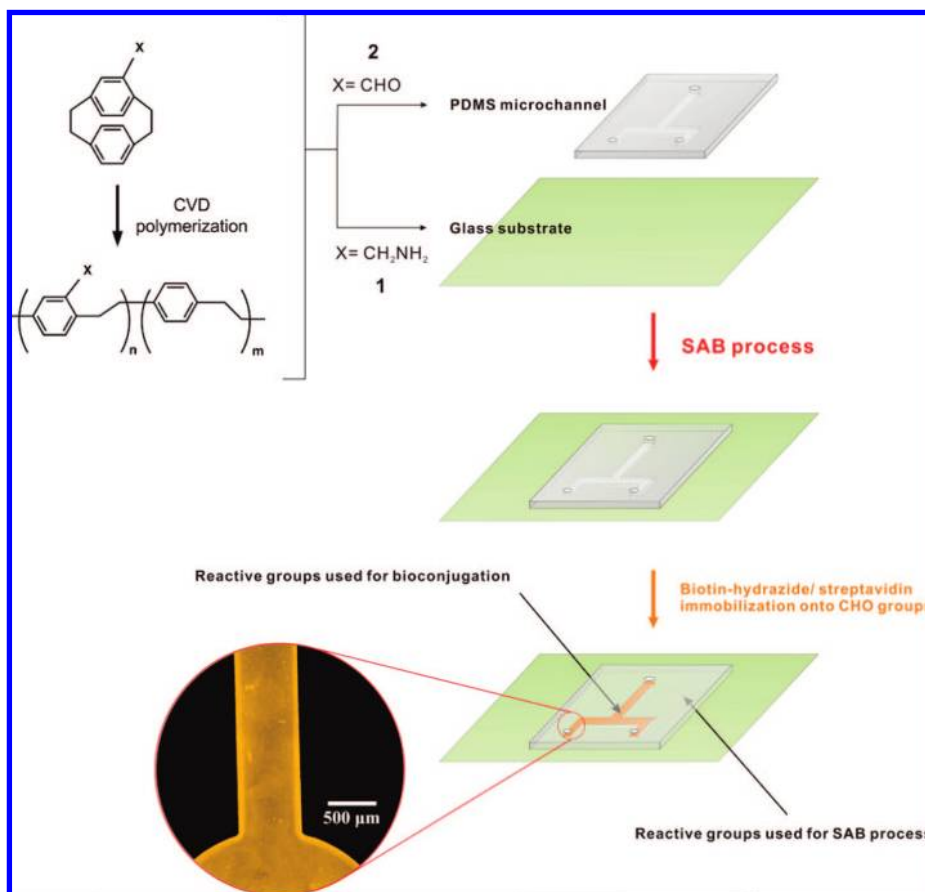


Figure 3. Process of dry adhesive bonding on microchannels by using CVD reactive coatings. The fluorescence micrograph (enlargement) is showing the biotin/TRITC–streptavidin modification on CVD polymer **2** within sealed microchannels after the dry adhesive bonding process.

because it undergoes nearly quantitative conversion with aldehyde groups and its interactions with streptavidin are known to result in tight confinement of streptavidin on the biotin-modified surface,^{33,40} which can be exploited for visualization of ligand binding. In a second step, we allowed TRITC-conjugated streptavidin to bind to the biotin immobilized onto the luminal surfaces of the microchannel. After rinsing with PBS buffer, the surfaces were inspected by fluorescence microscopy. The fluorescence micrograph of Figure 3 shows surface-modified microchannels that were coated with polymer **2** on the top and two side walls (PDMS-based surfaces) as well as polymer **1** on the bottom surface (glass slide) and then subjected to the biotin–streptavidin protocol. Homogenous distribution throughout the entire microchannel was observed, indicating that aldehyde groups were available throughout the entire luminal surface area. Because of the limited *z*-resolution of fluorescence microscopy, cross-sectional analysis was challenging, and this experiment cannot decidedly clarify whether the binding of biotin–streptavidin is specifically occurring on areas modified with polymer **2**. Reference experiments without biotin immobilization suggest that there are only low levels of nonspecific streptavidin adsorption in the absence of immobilized biotin, which is in accordance with previously reported data on patterned surface structures.^{32,34,36}

In order to address the simultaneous immobilization of two different biomolecules on top and bottom surfaces, we performed

a follow-up experiment involving two consecutive immobilization cycles.⁴¹ First, the microchannels were reacted with atto-655 NHS ester allowing covalent amide formation with polymer **1** modified surface (glass substrate, bottom). After a thorough rinse with buffer solution, subsequent biotin–streptavidin immobilization was performed according to a previously described procedure.⁴⁰ Confocal laser scanning microscopy was used to examine the resulting microchannels in details. As shown in Figure 4, top and side surfaces were associated with green color due to immobilized TRITC-labeled streptavidin present on surfaces modified with polymer **2**. The bottom surface had a red color due to covalent immobilization of a red-fluorescent atto-655 NHS ester via amino groups that originated from reactive coating **1**. The CLSM image reveals clearly distinguishable colors on the luminal surfaces associated with PDMS and glass, respectively. It should be noted that in spite of the additional complexity stemming from using a cascade of immobilization steps, excellent homogeneity throughout the entire channel, minimal nonspecific adsorption between different molecules (based on confocal microscopy), and excellent bonding strength (based on tensile stress testing) were observed.

CONCLUSIONS

In summary, we report a novel, solventless bonding approach for microfluidic devices that relies on a well-defined chemical reaction between two reactive polymer coatings with complemen-

(40) Chen, H. Y.; Elkasabi, Y.; Lahann, J. *J. Am. Chem. Soc.* **2006**, *128*, 374–380.

(41) Chen, H. Y.; Rouillard, J. M.; Gulari, E.; Lahann, J. *Proc. Natl. Acad. Sci. U.S.A.* **2007**, *104*, 11173–11178.

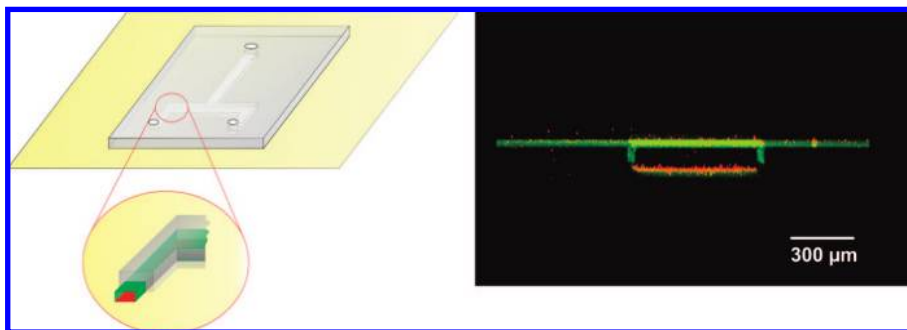


Figure 4. Left: illustration showing the distribution of fluorescence signals according to the ligands and dye used. The green color comprises TRITC-labeled streptavidin, which was immobilized according to the biotin–hydrazide presented on polymer **2** modified surfaces. The red surface in the bottom was formed by covalent immobilization of a red-fluorescent atto-655 NHS ester on the amino groups presented on the bottom surface that was modified by polymer **1**. Right: confocal micrograph showing the according fluorescence image of a sealed microchannel. The image was recorded by continuous image collection in the z-direction.

tary chemical groups. The polymeric reaction partners converted with high selectivity and close to quantitative yields and also showed excellent storage stability and low tendencies to undergo side reactions. Macromolecular reactants equipped with either amino or aldehyde groups were deposited onto substrates using a solventless CVD polymerization process that can be applied to a wide range of different substrate materials—thereby directly addressing substrate independence, a major need of many biotechnological applications. Moreover, bonding results in excellent adhesion of PDMS to a wide range of substrates including PDMS, glass, silicon, stainless steel, and PTFE with tensile strengths being higher than those measured for substrates bonded with plasma or UV/ozone treatment. The currently exploited temperatures of 140 °C are compatible with PDMS, PTFE, and many other polymers but clearly provide a challenge when materials such as polymethacrylate or polycarbonate ought to be used. Reducing the process temperature through process optimization and/or exploration of alternate bonding chemistries will therefore be an important direction of future work.

(42) Beebe, D. J.; Mensing, G. A.; Walker, G. M. *Annu. Rev. Biomed. Eng.* **2002**, *4*, 261–286.

Because this dry adhesion process is (i) independent of the chemical composition of the substrate, (ii) well-defined with respect to the bonding chemistry, (iii) can be controlled on demand, and (iv) can provide a biologically distinct binding platform, it may have important technological implications for miniaturized bioanalytical systems as well as microelectromechanical systems (MEMS) fabrication, where a substantial diversification of process materials is currently observed.^{1,17,42}

ACKNOWLEDGMENT

J.L. gratefully acknowledges support from the NSF in the form of a CAREER Grant (DMR-0449462) and funding from the NSF under the MRI program (DMR 0420785). This work is further supported by NSF (CHE-0449469, to Z.C.). We thank Professor Shuichi Takayama and Yaokuang Chung, University of Michigan, for the assistance with oxygen plasma bonding. We thank Professor Kotov, University of Michigan, for use of the ellipsometer. We gratefully acknowledge Dr. Shuji Ye for the ab initio calculation results.

Received for review February 18, 2008. Accepted March 31, 2008.

AC800341M